Received: 23 December 2019 | Revised: 30 April 2020 | Accepted: 5 June 2020

DOI: 10.1002/dac.4520

RESEARCH ARTICLE

WILEY

High-rate uncoded space-time labelling diversity with low-complexity detection

Sulaiman Saleem Patel[1] | **Tahmid Quazi**[2] | **Hongjun Xu**[2]

[1]Emerging Technology, Digital Consulting, KPMG Services (Pty.) Ltd., Durban, South Africa

[2]School of Engineering, University of Kwa-Zulu Natal, Durban, South Africa

Correspondence
Tahmid Quazi, School of Engineering, University of Kwa-Zulu Natal, Durban, South Africa.
Email: quazit@ukzn.ac.za

Summary

Uncoded space-time labelling diversity (USTLD) is a recent scheme that improved the error performance compared to conventional multiple-input, multiple-output systems. Thus far, USTLD has suffered from limited achievable data rates, as the original model uses only two transmit antennas. This motivates for the work in this paper, where the USTLD model is extended to allow for any desired number of transmit antennas. An analytical bound for the average bit error probability of this high-rate USTLD (HR-USTLD) system is derived. This expression is verified using the results of Monte Carlo simulations, which show a tight fit in the high signal-to-noise ratio region. The increased data rates associated with larger transmit antenna arrays in HR-USTLD systems come at the cost of increased detection complexity. Therefore, this paper studies the application of low-complexity detection algorithms based on the popular QR decomposition technique and proposes a new algorithm specifically designed for HR-USTLD systems. Analysis of this algorithm in terms of accuracy and computational complexity is also provided and benchmarked against maximum-likelihood detection (MLD). It is shown that the proposed algorithm achieves near-MLD accuracy, while reducing complexity by 79.75% and 92.53% for the respective 4×4 16QAM and 4×5 16PSK HR-USTLD systems investigated.

KEYWORDS

complexity analysis, detection algorithms, diversity techniques, labelling diversity, QR decomposition, wireless communication systems

1 | INTRODUCTION

1.1 | Context of research

The inclusion of diversity in wireless communication systems allows for many potential benefits, such as protection against burst errors and improved robustness in the presence of multipath fading or co-channel interference.[1] Uncoded space-time labelling diversity (USTLD)[2-5] is a recent scheme which achieves three levels of diversity: antenna diversity, time diversity and labelling diversity. Antenna diversity is achieved by adopting a multiple-input, multiple-output (MIMO) system model. The inclusion of multiple antennas at both the transmitter and receiver generates more signal paths, increasing the likelihood of correct detection.[1,6] The original work on USTLD describes a MIMO system of two transmit antennas and any arbitrary N_{Rx} receive antennas.[2] To achieve time diversity, symbols representing the same

binary data are transmitted in two time slots. To achieve labelling diversity, symbols are selected from constellations with different binary mappings in each time slot. The design and selection of mappers aims to maximise the minimum product Euclidean distance (ED) between symbol pairs in each constellation. Stated differently, adjacent symbols in the constellation defined by the primary mapper are spaced further apart in the constellations defined by subsequent mappers. By following this approach, detection is done based on symbol pairs, instead of individual symbols. Due to difficulties in designing labelling diversity mappers, Xu et al[2] constrained their studies to M-ary quadrature amplitude modulation (MQAM) and M-ary phase shift keying (MPSK) modulation schemes. The challenge of labelling diversity mapper design for other modulation schemes has also been explored in related works.[3,5]

A drawback of the USTLD scheme is that transmitting symbols containing the same information across two time slots halves the effective data rate of the system. In general, the two approaches to improving the data rate of uncoded MIMO systems, such as USTLD, are to either increase the modulation order, M, or to increase the number of transmission streams. Higher modulation orders allow the system to transmit larger codewords in each instance, that is, the number of bits per codeword is increased. To increase the number of transmission streams, MIMO systems typically increase the number of transmit antennas, N_{Tx}, and transmit independent symbols from each antenna simultaneously.[1,6] This increases the number of codewords transmitted during a single time slot. It is possible to increase either M or N_{Tx} in USTLD systems; however, they also result in increasing the complexity of detection for receiver hardware. The algorithmic complexity of performing maximum-likelihood detection (MLD or ML detection) on an $N_{\mathrm{Tx}} \times N_{\mathrm{Rx}}$ USTLD system with modulation order M is $\mathcal{O}\left(N_{\mathrm{Tx}} N_{\mathrm{Rx}} M^{N_{\mathrm{Tx}}}\right)$, where $\mathcal{O}(\cdot)$ is the 'order of' operator used in complexity analysis.[7] This is derived in the Appendix of this paper in terms of real operations, the metric suggested by Pillay and Xu.[4] The high complexity of MLD motivates for the development of low-complexity detection algorithms (LCDAs), with the goal of achieving near-ML accuracy at significantly reduced complexity.[8]

The current work on USTLD systems[2] only allows for increasing the data rate by using higher modulation orders, as N_{Tx} in the system is fixed at only two transmit antennas. This is because the original USTLD system model[2] was conceived as a direct extension of the Alamouti space-time block code[9] to improve its bit error rate (BER). Since the structure proposed by Alamouti constrains the system to only two transmit antennas,[9] the same constraint was applied to the original USTLD model.[2]

However, as discussed in literature,[1,6] the data rate of uncoded MIMO systems increases logarithmically with M and linearly with N_{Tx}. Thus, the improvement in data rate as M increases is hyperbolic and becomes negligible as $M \to \infty$. By contrast, increasing N_{Tx} provides constant data rate improvement. Another drawback to increasing modulation order is that the average ED between constellation points for normalised constellations decreases as M increases, resulting in inferior error performance. It is also noted that increasing the modulation order above $M = 16$ presents difficulties in designing optimal mappers to achieve labelling diversity.[2,3,10] For these reasons, this paper proposes to increase the achievable data rates of USTLD systems by extending the existing model to allow for more than two transmit antennas. To distinguish between such a system and the existing USTLD model, this paper adopts the term 'high-rate USTLD' (HR-USTLD) to describe the $N_{\mathrm{Tx}} \times N_{\mathrm{Rx}}$ USTLD model proposed. It is further noted that Ayanda et al[11] have also extended the original USTLD model to allow for the use of three transmit antennas and three labelling diversity mappers. However, the system proposed by Ayanda et al also uses a third transmission time slot and thus achieves the same data rate as the original USTLD model.[2,11] Thus, the HR-USTLD system presented in this paper is capable of achieving higher data rates than the three mapper USTLD system.

As mentioned previously, HR-USTLD incurs high detection complexity. Existing LCDAs for MIMO systems may be divided into two broad classes: linear detection schemes and search-based detection schemes. Linear detection schemes, such as zero forcing[12] and minimum mean squared error equalising,[13] perform linear matrix operations during the detection process, incurring a lower complexity cost than MLD. However, these schemes are unable to fully capture the receive diversity of the MIMO system, leading to reduced detection accuracy and a degradation in error performance.[14,15] For this reason, this paper focuses on applying search-based LCDAs to the systems investigated.

Search-based detection schemes are often based on QR decomposition (QRD), which transforms the detection problem into a tree search. In this way, detection is done one information codeword at a time. Spherical detection (SD)[16,17] is a popular scheme that has been combined with QRD to reduce complexity. This is achieved by constraining the search space at each layer of the search to only those symbols within a predefined hypersphere of the received signal. Another important improvement to the standard QRD approach is QRD-m, where the m best paths are considered while traversing the search tree.[18] In the work by Radosavljevic et al,[19] a technique that is referred to in this paper as the QR-QL Parallel Searching Algorithm (QRLPSA) was proposed. This technique reduces the complexity of QRD with SD by simultaneously considering the equivalent QL decomposition (QLD) search tree. The QRD search tree is based

on an upper, right triangular structure, whereas the QLD search tree is based on a lower, left triangular structure. As such, the order in which symbols are detected is reversed depending on the search tree structure used. By performing partial, parallel searches through both trees, only half of each individual tree need be traversed to obtain estimates for all symbols. The QRLPSA has been extended by Peer et al,[20] whose algorithm introduces two additional detection stages. The first additional stage involves merging the m partial candidate symbol vectors obtained from the QR and QL search trees, respectively, and pruning these to only the K best candidate vectors. The second additional stage is to search through these K candidate vectors, using either the QR or QL search tree, and generate an ML-hypothesis candidate vector. A set of counter-hypotheses is generated, and the log-likelihood ratio (LLR) between the ML-hypothesis and each of the counter-hypotheses is then computed, after which the suitability of the ML hypothesis is determined.

In this paper, USTLD is extended from the $2 \times N_{\mathrm{Rx}}$ model originally proposed by Xu et al[2] to a more general $N_{\mathrm{Tx}} \times N_{\mathrm{Rx}}$ HR-USTLD model. Increasing the number of transmit antennas allows for higher data rates to be achieved. Alternatively, a desired data rate can be obtained by using more transmit antennas and a lower modulation order. This is desirable, as many existing mapper design techniques for labelling diversity systems do not perform well when scaled to higher order modulations.[3,5] In other works on USTLD,[21,22] a search-based LCDA based on performing an orthogonal projection has been proposed. However, the manner in which this LCDA is presented is only valid for two transmit antennas. For this reason, this paper further proposes a new LCDA for HR-USTLD which removes this constraint and is based on the QRLPSA[19] and its extension.[20] It is shown that the proposed LCDA is capable of achieving ML performance at significantly reduced complexity. It should be noted that the SD approach is not applicable to USTLD and HR-USTLD due to the manner in which mappers are designed to achieve labelling diversity and that the use of LLRs is not feasible for uncoded systems such USTLD and HR-USTLD.[23]

1.2 | Structure and notation

The remainder of this paper is structured as follows. In Section 2, the system model for HR-USTLD is given. Section 2.1 describes the transmission model, and Section 2.2 describes the various detection schemes which may be applied—including ML detection, existing LCDAs and the proposed LCDA for this paper. Section 3 provides analytical expressions to evaluate the proposed system. Section 3.1 derives the analytical average bit error probability (ABEP), and Section 3.2 gives analytical expressions to evaluate and compare the algorithmic complexity of the detection algorithms given in Section 2.2. Section 4 provides and discusses the results obtained through Monte Carlo simulations, and finally, Section 5 concludes this paper.

The notation used in this paper is to denote vectors in boldface, matrices in italicised boldface, and scalars in italics. Occasionally, two levels of subscripts are used when referring to elements of a matrix or vector during a particular time slot. In these cases, the inner subscript refers to the position of the element within the matrix and the outer subscript refers to the time slot considered. For example, V_{3_2} is read as the third element of vector $\mathbf{V}$ during the second time slot. The operators $\mathcal{E}\{\cdot\}$, $\|\cdot\|$, $\lfloor\cdot\rfloor$, $\lceil\cdot\rceil$, $(\cdot)^{\mathrm{H}}$, and $(\cdot)^{\mathrm{T}}$ denote the statistical expectation, Frobenius vector norm, floor, ceiling, Hermitian, and matrix transpose, respectively. Sets of variables are denoted in braces, and a superscript outside the braces indicates the size of the set. The operator $|\cdot|$ represents either the magnitude of a complex number or the cardinality of a set, depending on the argument used.

1.3 | Contributions

The original contributions of this article are as follows:

1. The achievable data rates of USTLD systems are increased by employing a HR-USTLD transmission model with any arbitrary N_{Tx} transmit antennas. A tight, closed-form union bound expression for the ABEP of HR-USTLD systems is presented.
2. A comprehensive study of the application of existing QRD-based LCDAs to HR-USTLD systems is conducted. Each of these LCDAs was originally proposed for systems that do not achieve labelling diversity; hence, they have been adapted for USTLD systems. It is noted that the only previously proposed LCDA for USTLD systems[21,22] cannot be applied to HR-USTLD systems as it fails when used with more than two transmit antennas.

3. A new LCDA designed specifically for HR-USTLD systems is proposed, which achieves significantly higher detection accuracy when compared to the existing LCDAs studied (i.e. QRD, QRD-m, QRLPSA, and extended QRLPSA).
4. New insights on the manner in which labelling diversity affects the BER performance of systems are presented. These were not reported in the original work on USTLD systems.[2]
5. Expressions are derived to quantitatively evaluate the computational complexity for all detection algorithms presented in this paper.

2 | SYSTEM MODEL

2.1 | Transmission model

This paper considers an $N_{\mathrm{Tx}} \times N_{\mathrm{Rx}}$ HR-USTLD system, where the number of transmit antennas is constrained such that $N_{\mathrm{Tx}} \leq N_{\mathrm{Rx}}$. A stream of $N_{\mathrm{Tx}}\, log_2 M$ information bits is transmitted over two time slots. These bits are grouped into N_{Tx} labels denoted by vector $\mathbf{B} = [B_1 \ldots B_{N_{\mathrm{Tx}}}]^{\mathrm{T}}$, where the term 'label' is for the $log_2 M$ consecutive bits from the information bitstream. To achieve labelling diversity, in each time slot, transmitted symbols are selected from constellations with different mappings. The constellation mapper used in the t-th time slot, where $t \in [1:2]$, is denoted Ω_t.

$N_{\mathrm{Tx}} \times 1$ transmit symbol vector $\mathbf{x}_t = \left[x_{1_t} \ldots x_{N_{\mathrm{Tx}t}}\right]^{\mathrm{T}}$ is generated such that $x_{i_1} = \Omega_1(B_i)$ and $x_{i_2} = \Omega_2(B_i)$, where $i \in [1 : N_{\mathrm{Tx}}]$. The set of M possible symbol pairs is denoted ξ, such that its j-th entry $\xi^{(j)}$ is given by $\xi^{(j)} = \langle \Omega_1(j-1), \Omega_2(j-1) \rangle$, where $j \in [1:M]$. By simultaneously sending independent symbols from each transmit antenna, the HR-USTLD achieves spatial multiplexing in a similar manner to the Vertical-Bell Laboratories Layered Space-Time (V-BLAST) architecture.[24]

After transmission, the $N_{\mathrm{Rx}} \times 1$ received signal vector, $\mathbf{y}_t$, transmitted in the t-th time slot, is given by

$$\mathbf{y}_t = \sqrt{\frac{\gamma}{N_{\mathrm{Tx}}}}\mathbf{H}_t\mathbf{x}_t + \mathbf{n}_t; \langle x_{i_1}, x_{i_2} \rangle \in \xi, i \in [1 : N_{\mathrm{Tx}}]. \tag{1}$$

In Equation (1), γ represents the total average signal-to-noise ratio (SNR) of the transmission, assumed to be equally distributed among the N_{Tx} transmit antennas. $\boldsymbol{H}_t$ is the $N_{\mathrm{Rx}} \times N_{\mathrm{Tx}}$ matrix of channel coefficients. These channels are assumed to follow a Rayleigh amplitude distribution of zero mean and unit variance, the probability density function of which is $f_{\mathrm{Rayleigh}}(\alpha) = \alpha e^{-0.5\alpha^2}$, where α is the fading amplitude. Furthermore, channels are assumed to be frequency flat and fast-fading. $N_{\mathrm{Rx}} \times 1$ vector $\mathbf{n}_t$ represents additive white Gaussian noise (AWGN) which follows a complex normal distribution with zero mean and variance $\sigma_{\mathrm{n}}^2 = \frac{N_0}{2}$ per dimension. Both the fading channels and AWGN have uniform phase distribution.

The design of a suitable pair of mappers ($\Omega_t, t \in [1:2]$) affects the extent to which the USTLD system achieves labelling diversity, and hence, its error performance. When designing a pair of mappers, the objective is to ensure that the labels corresponding to neighbouring points when mapped by Ω_1 are spaced further apart when mapped by Ω_2. Techniques to design mappers for USTLD systems is an ongoing research area,[2,3,5,10,25] and is beyond the scope of this paper. Thus, the constellations studied are constrained to those for which mapper designs are readily obtainable from literature.[2,10,25]

Based on the original work on USTLD systems[2] and the study by Samra et al,[10] it is optimal to choose a Gray-coded mapping for Ω_1. Ω_2 then requires a different mapper to be selected. In this paper, for the case of 16QAM, the mapper proposed by Samra et al,[10] found to be optimal by previous works on labelling diversity systems,[2,10] is used. These constellation mappings are illustrated in Figure 1. However, the optimal mapper design technique used by Samra et al[10] is only feasible for up to 16-ary constellation sizes. Therefore, for 64QAM, the heuristic-based mapper design proposed by Seddik et al[25] is used. This heuristic design was found to be superior to the 64QAM mapper design presented by Xu et al[2] in other works on USTLD systems.[3] For the case of MPSK constellations, the secondary mapper is constructed by swapping alternate symbols with their diagonally opposite counterparts, as suggested by Xu et al.[2] All constellations are power normalised such that $\mathcal{E}\{|x_{i_t}|^2\} = 1$, where $i \in [1 : N_{\mathrm{Tx}}]$ and $t \in [1:2]$.

The proposed HR-USTLD model achieves a data rate of $0.5 N_{\mathrm{Tx}} log_2 M$ bits/s/Hz. This expression is in agreement with the explanation given in Section 1, where it is mentioned that the data rate of uncoded MIMO systems increases logarithmically with M and linearly with N_{Tx}. Thus, the improvement in data rate as M increases is hyperbolic and becomes negligible as $M \to \infty$. By contrast, increasing N_{Tx} provides constant data rate improvement.

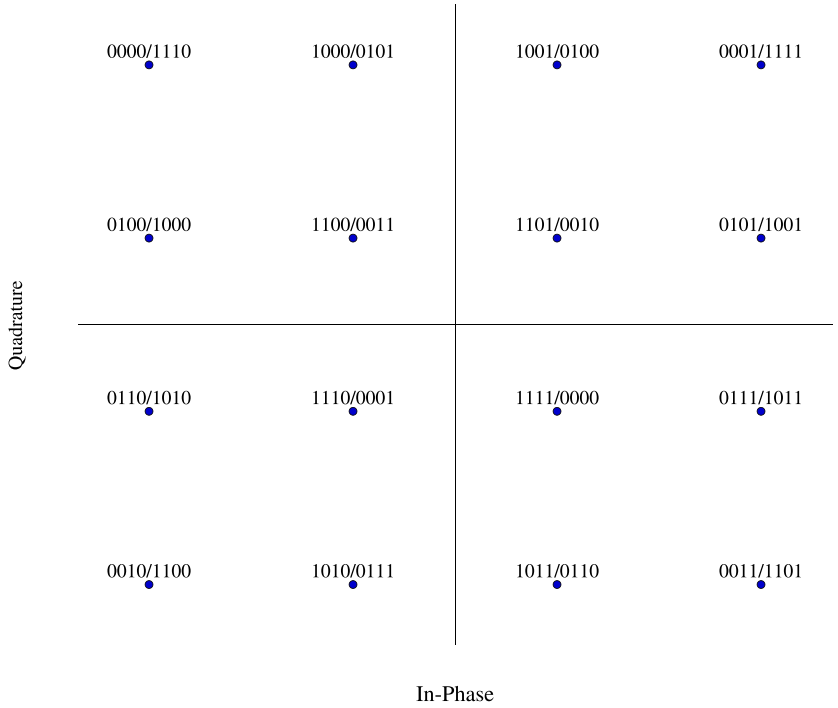

FIGURE 1 16-QAM binary constellation mapping, key: Ω_1/Ω_2

2.2 | Detection model

In this work, different detection algorithms are implemented and compared in terms of accuracy and complexity.

Detection is performed by first dividing (1) by the SNR factor to produce

$$\mathbf{z}_t = \sqrt{\frac{N_{\mathrm{Tx}}}{\gamma}}\,\mathbf{y}_t = \mathbf{H}_t\mathbf{x}_t + \acute{}\mathbf{n}_t, \tag{2}$$

where the equivalent noise term $\acute{}\mathbf{n}_t$ is defined as $\acute{}\mathbf{n}_t = \sqrt{\frac{N_{\mathrm{Tx}}}{\gamma}}\mathbf{n}_t$. All detection techniques investigated assume that perfect channel state information is available at the receiver. After detecting the transmitted symbol pairs, decoding is done to recover the associated labels and hence, the transmitted information.

2.2.1 | Maximum likelihood detection

MLD is the benchmark detection technique investigated in this paper. To perform MLD on the proposed HR-USTLD system, it is required that received symbol vectors from both time slots are considered simultaneously. Unlike conventional MIMO detection, MLD for labelling diversity is concerned with joint detection using corresponding symbols from both mappers. As such, the output of the ML detector is two $N_{\mathrm{Tx}} \times 1$ symbol vectors, $\tilde{\mathbf{x}}_1$ and $\tilde{\mathbf{x}}_2$. The detected data are represented by the label vector, $\tilde{\mathbf{B}}$, which corresponds to the labels associated with the pair $\langle \tilde{\mathbf{x}}_1, \tilde{\mathbf{x}}_2 \rangle$. The MLD search based on Equation (2) is described by

$$\langle \tilde{\mathbf{x}}_1, \tilde{\mathbf{x}}_2 \rangle = \underset{\substack{\langle \hat{x}_{j_1}, \hat{x}_{j_2} \rangle \in \xi \\ j \in [1:N_{\mathrm{Tx}}]}}{\arg\min} \mathcal{A}(\hat{\mathbf{x}}_1, \hat{\mathbf{x}}_2), \tag{3}$$

where the MLD detection metric $\mathcal{A}$ is defined as

$$\mathcal{A}(\hat{\mathbf{x}}_1, \hat{\mathbf{x}}_2) = \|\mathbf{z}_1 - \mathbf{H}_1\hat{\mathbf{x}}_1\|^2 + \|\mathbf{z}_2 - \mathbf{H}_2\hat{\mathbf{x}}_2\|^2. \tag{4}$$

MLD incurs high complexity but ensures the most accurate results, as there are $M^{N_{\mathrm{Tx}}}$ candidate symbol pairs that need to be considered.

2.2.2 | Standard QRD and QRD-m

QRD and QLD are two techniques for decomposing an arbitrary complex-valued matrix, $\boldsymbol{A}$, into an equivalent matrix product. The QRD of $\boldsymbol{A}$ is defined as $\boldsymbol{A} = \boldsymbol{Q}_{\mathrm{QR}}\boldsymbol{R}$, and similarly the QLD of $\boldsymbol{A}$ is $\boldsymbol{A} = \boldsymbol{Q}_{\mathrm{QL}}\boldsymbol{L}$. $\boldsymbol{Q}_{\mathrm{QR}}$ and $\boldsymbol{Q}_{\mathrm{QL}}$ are unitary, complex orthogonal matrices such that $\left(\mathbf{Q}_{\mathrm{QR}}\right)^{\mathrm{H}}\mathbf{Q}_{\mathrm{QR}} = \left(\mathbf{Q}_{\mathrm{QL}}\right)^{\mathrm{H}}\mathbf{Q}_{\mathrm{QL}} = \mathbf{I}$; where $\boldsymbol{I}$ is the identity matrix. $\boldsymbol{R}$ is an upper, right triangular matrix, and $\boldsymbol{L}$ is a lower, left triangular matrix.

To apply these techniques to detection in MIMO systems, the channel coefficient matrix, $\boldsymbol{H}$, is first decomposed. Thereafter, Equation (2) is left-multiplied by the Hermitian of the unitary matrix to produce Equation (5) for QRD, and Equation (6) for QLD.

$$\boldsymbol{\alpha}_t = \left(\mathbf{Q}_{\mathrm{QR}_t}\right)^{\mathrm{H}}\mathbf{z}_t = \mathbf{R}_t\mathbf{x}_t + \left(\mathbf{Q}_{\mathrm{QR}_t}\right)^{\mathrm{H}}\mathbf{n}_t \tag{5}$$

$$\boldsymbol{\beta}_t = \left(\mathbf{Q}_{\mathrm{QL}_t}\right)^{\mathrm{H}}\mathbf{z}_t = \mathbf{L}_t\mathbf{x}_t + \left(\mathbf{Q}_{\mathrm{QL}_t}\right)^{\mathrm{H}}\mathbf{n}_t \tag{6}$$

Due to the triangular structure of matrices $\boldsymbol{R}$ and $\boldsymbol{L}$, detection may be performed on a row-by-row basis starting with the row with the most zero elements (i.e. the N_{Tx}-th row of $\boldsymbol{R}$ and the first row of $\boldsymbol{L}$). Back-substitution is then used, so that in each row, there are only M candidate symbol pairs that must be tested. This allows the detection to be formulated as a tree search, through N_{Tx} layers, with M candidate nodes per layer. Each node represents a candidate label, and its associated symbol pair generated from Ω_1 and Ω_2. The simplest case of QRD and QLD is when the system of equations defined by Equations (5) and (6) is perfectly determined. This is the case if the decomposed matrix, $\boldsymbol{H}$, was a square matrix (i.e. $N_{\mathrm{Tx}} = N_{\mathrm{Rx}}$). Figure 2 illustrates the QRD search tree for a perfectly determined system. Searching begins at the N_{Tx}-th row of matrix $\boldsymbol{R}$ and ends at its first row. Without loss of generality, it is assumed that Node $M-1$ is detected from Row N_{Tx} and Node 1 is detected from Row $N_{\mathrm{Tx}}-1$ to illustrate expansion of nodes during the search.

If $\boldsymbol{H}$ is not a square matrix, QRD and QLD may still be performed. When $\boldsymbol{H}$ has fewer rows than columns (i.e. $N_{\mathrm{Tx}} < N_{\mathrm{Rx}}$), the system of equations it represents is overdetermined. After decomposition, the triangular matrix of an overdetermined system has rank N_{Tx} and $N_{\mathrm{Rx}} - N_{\mathrm{Tx}}$ zero rows. The case of $\boldsymbol{H}$ having more rows than columns (i.e $N_{\mathrm{Tx}} > N_{\mathrm{Rx}}$), does not arise due to the constraints placed on the system.

If all zero rows of any overdetermined system are discarded, the q-th rows of Equations (5) and (6), during the t-th time slot, are given by the scalar equations:

$$\alpha_{q_t} = \sum_{i=q}^{N_{\mathrm{Tx}}} r_{q,i_t} x_{i_t}, \tag{7}$$

$$\beta_{q_t} = \sum_{i=1}^{q} l_{q,i_t} x_{i_t}. \tag{8}$$

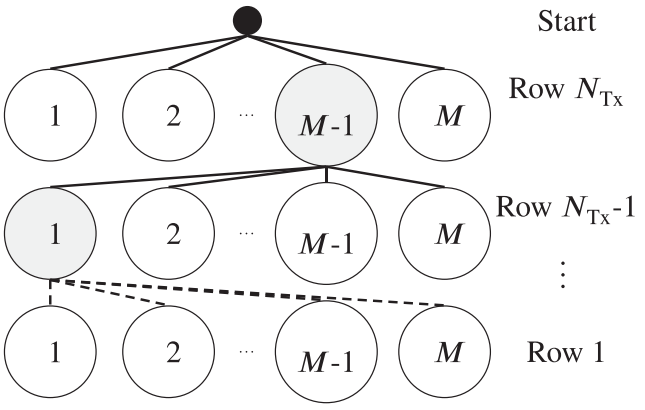

FIGURE 2 Illustration of a QR decomposition (QRD) search tree

The row-by-row detection adapted from Equation (3) and based on Equation (7) for the q-th row of a QRD search is then given by

$$\left\langle \tilde{x}_{q_1}, \tilde{x}_{q_2} \right\rangle = \underset{\langle \hat{x}_1, \hat{x}_2 \rangle \in \xi}{\arg\min} \sum_{t=1}^{2} \left| \alpha_{q_t} - r_{q,q_t} \hat{x}_t - S_{1_t} \right|^2, \tag{9}$$

and likewise, for the q-th row of a QLD search, the row-by-row detection based on Equation (8) is

$$\left\langle \tilde{x}_{q_1}, \tilde{x}_{q_2} \right\rangle = \underset{\langle \hat{x}_1, \hat{x}_2 \rangle \in \xi}{\arg\min} \sum_{t=1}^{2} \left| \beta_{q_t} - S_{2_t} - l_{q,q_t} \hat{x}_t \right|^2, \tag{10}$$

where the summation terms are defined as

$$S_{1_t} = \sum_{i=q+1}^{N_{\mathrm{Tx}}} r_{q,i_t} \tilde{x}_{i_t}, \tag{11}$$

$$S_{2_t} = \sum_{i=1}^{q-1} l_{q,i_t} \tilde{x}_{i_t}. \tag{12}$$

It may be intuitively observed that both QRD and QLD are equivalent techniques. Radosavljevic et al[19] has previously shown that performing QRD on a column-reversed channel matrix $\mathbf{H}^{\mathrm{rev}} = [\mathbf{h}_{N_{\mathrm{Tx}}} \ldots \mathbf{h}_1]$ produces a decomposition equivalent to the QLD of the original channel matrix $\boldsymbol{H}$, where $\mathbf{h}_i$ represents the i-th column of the un-reversed channel matrix $\boldsymbol{H}$.

A drawback of standard QRD detection is that it is susceptible to error propagation through the search tree due to the use of back-substitution. Referring to Figure 2, suppose an error occurs in Row N_{Tx} and correct detection should have yielded Node 1. This incorrect detection then increases the likelihood of a detection error in all rows from Row $N_{\mathrm{Tx}} - 1$ to Row 1. An approach to combat this is to change the detection order to maximise the probability of correct detection in upper rows of the search tree.[26] A simple method of achieving this is by preprocessing and reordering the columns of $\boldsymbol{H}$. Columns are arranged such that the sum of column-norms from both time slots are in ascending order, and the rows of $\mathbf{x}$ are also reordered accordingly. For example, assuming a $5 \times N_{\mathrm{Rx}}$ HR-USTLD system described according to Equation (2) by

$$\mathbf{z}_t = [\mathbf{h}_1\, \mathbf{h}_2\, \mathbf{h}_3\, \mathbf{h}_4\, \mathbf{h}_5]_t \begin{bmatrix} x_1 \\ x_2 \\ x_3 \\ x_4 \\ x_5 \end{bmatrix}_t + \acute{\mathbf{n}}_t. \tag{13}$$

Ordering is done according to the sum of column-norms across time slots $t = 1$ and $t = 2$. Without loss of generality, assume that it is found that $\sum_{t=1}^{2} \|\mathbf{h}_3\|_t^2 < \sum_{t=1}^{2} \|\mathbf{h}_1\|_t^2 < \sum_{t=1}^{2} \|\mathbf{h}_5\|_t^2 < \sum_{t=1}^{2} \|\mathbf{h}_4\|_t^2 < \sum_{t=1}^{2} \|\mathbf{h}_2\|_t^2$. This means that the probability of correctly detecting x_2 is highest, and the probability of erroneously detecting x_3 is highest. Reordering Equation (13) accordingly for QRD produces

$$\mathbf{z}_t = [\mathbf{h}_3\, \mathbf{h}_1\, \mathbf{h}_5\, \mathbf{h}_4\, \mathbf{h}_2]_t \begin{bmatrix} x_3 \\ x_1 \\ x_5 \\ x_4 \\ x_2 \end{bmatrix}_t + \acute{\mathbf{n}}_t. \tag{14}$$

Due to the upper, right triangular structure of $\boldsymbol{R}$ after decomposition, it is evident that detection is now done in order of descending $\sum \|\mathbf{h}\|^2$. Similarly, the appropriate reordering for QLD is

$$\mathbf{z}_t = [\mathbf{h}_2\, \mathbf{h}_4\, \mathbf{h}_5\, \mathbf{h}_1\, \mathbf{h}_3]_t \begin{bmatrix} x_2 \\ x_4 \\ x_5 \\ x_1 \\ x_3 \end{bmatrix}_t + \acute{\mathbf{n}}_t. \tag{15}$$

Another improvement to standard QRD, presented by Kim et al,[18] is QRD-m detection. In QRD-m, the best m nodes are expanded at each level of the search tree, where $m \in [1 : M]$. The case of $m = 1$ is identical to the standard QRD approach. In QRD-m, the cumulative metrics are considered at each search layer. QRD-m is illustrated with $m = 2$ on a perfectly determined system in Figure 3.

2.2.3 | QR-QL parallel searching

The QRLPSA[19] takes advantage of the symmetry of matrices $\boldsymbol{R}$ and $\boldsymbol{L}$ to reduce the number of layers to be searched through when performing detection. If the channel matrix of an HR-USTLD system is decomposed using the QRD approach, the order in which labels are detected starts from label $B_{N_{\mathrm{Tx}}}$ and ends at label B_1. If the QLD approach is used, this order is reversed. It may be observed from Equations (9) and (10) that the latter layers of either search tree have more terms to be computed when performing detection.

QRLPSA exploits the similar structure of the search trees obtained via QRD and QLD. By evaluating only the first $\left\lfloor \frac{N_{\mathrm{Tx}}}{2} \right\rfloor$ layers of each search tree in parallel, the QLD search tree is able to detect labels B_1 to $B_{\left\lfloor \frac{N_{\mathrm{Tx}}}{2} \right\rfloor}$, and the QRD search tree is able to detect labels $B_{N_{\mathrm{Tx}} - \left\lfloor \frac{N_{\mathrm{Tx}}}{2} \right\rfloor + 1}$ to $B_{N_{\mathrm{Tx}}}$.

In general, for the case of even N_{Tx}, the floor operator is redundant and thus by parallel searching through the first $\frac{N_{\mathrm{Tx}}}{2}$ layers of both search trees, an estimate for $\mathbf{B}$ can be obtained. In the case of odd N_{Tx}, the $\left\lceil \frac{N_{\mathrm{Tx}}}{2} \right\rceil$-th layer remains after parallel searching. This requires that either the QRD or QLD search tree be expanded by one extra layer. The original work by Radosavljevic et al[19] also uses multiple search paths, as in QRD-m. It further makes use of reordering the matrix $\boldsymbol{H}$ such that the outermost columns have the highest summed column-norms. To illustrate this, consider the example system given in Section 2.2.2 and Equations (13)–(15). Reordering Equation (13) to perform parallel searching produces

$$\mathbf{z}_t = [\mathbf{h}_2\, \mathbf{h}_5\, \mathbf{h}_3\, \mathbf{h}_1\, \mathbf{h}_4]_t \begin{bmatrix} x_2 \\ x_5 \\ x_3 \\ x_1 \\ x_4 \end{bmatrix}_t + \acute{\mathbf{n}}_t. \tag{16}$$

In this way, the QLD search tree is marginally more accurate than the QRD search tree, which suggests that the remaining layer after parallel searching be obtained by expanding one more layer of the QLD search tree.

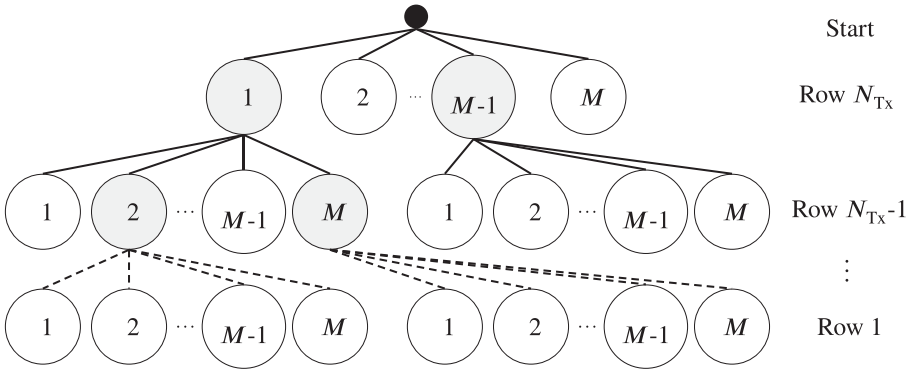

FIGURE 3 Illustration of a QR decomposition (QRD-m) search tree

2.2.4 | Extended QR-QL parallel searching algorithm

An extension to the QRLPSA was proposed by Peer et al,[20] where two further stages are introduced to the detection process. Peer et al[20] developed their algorithm for a coded system—as such, only the aspects applicable to uncoded systems such as HR-USTLD are investigated further in this paper.

The three stage structure of the uncoded aspects of extended QRLPSA is illustrated in Figure 4. The first stage is to perform parallel searching as in the QRLPSA, which produces m partial candidate label vectors from the QRD and QLD search trees, respectively, denoted $\{\tilde{\mathbf{B}}\}_{\mathrm{QR}}^{m}$ and $\{\tilde{\mathbf{B}}\}_{\mathrm{QL}}^{m}$. The second stage is to merge these partial candidate symbol pair vectors to form a set of m^2 candidate symbol pair vectors, denoted ξ_{merged}, for which the corresponding set of labels are $\{\tilde{\mathbf{B}}\}^{m^2}$ such that

$$\xi_{\mathrm{merged}} = \left\langle \Omega_1\left(\{\tilde{\mathbf{B}}\}^{m^2}\right), \Omega_2\left(\{\tilde{\mathbf{B}}\}^{m^2}\right)\right\rangle. \tag{17}$$

The detection metrics of the partial candidate vectors are summed to produce a detection metric for the merged candidate vectors. This set is then reduced to a set of K candidate labels, $\{\tilde{\mathbf{B}}\}^{K} \subset \{\tilde{\mathbf{B}}\}^{m^2}$, where $K \in [1 : m^2)$. $\{\tilde{\mathbf{B}}\}^{K}$ is then populated with the K candidate label vectors from $\{\tilde{\mathbf{B}}\}^{m^2}$ with the lowest merged detection metrics and defines candidate symbol vector pairs

$$\xi_{\mathrm{reduced}} = \left\langle \Omega_1\left(\{\tilde{\mathbf{B}}\}^{K}\right), \Omega_2\left(\{\tilde{\mathbf{B}}\}^{K}\right)\right\rangle. \tag{18}$$

In the final stage, a QLD tree search through only ξ_{reduced} is performed, yielding the final estimate of the transmitted labels. The detection metric for the q-th layer of this search is given by Equation (19), where $q \in [1 : N_{\mathrm{Tx}}]$. This metric has been obtained by modifying Equation (10). Thereafter, Peer et al[20] make use of techniques applicable to coded systems to determine the suitability of this estimate; however, these further techniques are not applicable for HR-USTLD.

$$\left\langle \tilde{x}_{q_1}, \tilde{x}_{q_2}\right\rangle = \underset{\langle \hat{x}_1, \hat{x}_2\rangle \in \xi_{\mathrm{reduced}}}{\arg\min} \sum_{t=1}^{2} \left| \beta_{q_t} - \sum_{i=1}^{q-1} l_{q,i_t} \tilde{x}_{i_t} - l_{q,q_t} \hat{x}_t \right|^2 \tag{19}$$

2.2.5 | Proposed LCDA: MSRSD-USTLD

As shown by the results in Section 4, the extended QRLPSA[20] does not improve detection accuracy compared to QRLPSA[19] when applied to HR-USTLD. It is also shown that both these algorithms offer poor detection accuracy compared to MLD, with a loss of up to 7 dB in the high SNR region of the systems investigated (see Figures 8A and 9A and).

There is generally a trade-off between accuracy and complexity in LCDAs. The QRD-based LCDAs presented reduce complexity by transforming the exhaustive ML search to a layer-by-layer tree search, which reduces the search space of candidate symbol vector pairs considered. However, adopting a layer-by-layer approach reduces the amount of information used to perform detection at each stage of the tree search, which results in these LCDAs being unable to fully capture the diversity of the system.[27] This is further motivated by the results in Figures 8A and 9A and. By considering more received signals during detection, such as when computing ML metric $\mathcal{A}$ in Equation (4), more information about the channel is present to increase detection accuracy. Moreover, QRD-based LCDAs are susceptible to error propagation through the search tree, which leads to severe consequences if there is a detection error in earlier layers of the search tree.

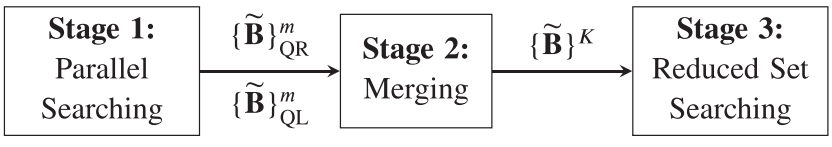

FIGURE 4 Block diagram of extended QR-QL Parallel Searching Algorithm (QRLPSA)

In order to improve the accuracy of extended QRLPSA, this paper proposes a new scheme called MSRSD-USTLD. The proposed scheme follows the same three-stage structure as extended QRLPSA (shown in Figure 4), but increases accuracy by considering a greater search space than extended QRLPSA during the final stage of detection. In addition, the final reduced search set for MSRSD-USTLD is based on the ML metric, $\mathcal{A}$, instead of the QLD tree search used in extended QRLPSA. This further increases accuracy but also causes an increase in complexity. A more detailed block diagram of MSRSD-USTLD is given in Figure 5.

The first two stages of MSRSD-USTLD are logically the same as for the extended QRLPSA. Parallel searching is performed during Stage 1 to obtain partial candidate label vectors $\{\tilde{\mathbf{B}}\}_{\mathrm{QR}}^{m}$ and $\{\tilde{\mathbf{B}}\}_{\mathrm{QL}}^{m}$, which are merged and reduced during Stage 2 to produce $\{\tilde{\mathbf{B}}\}^{m^2}$, ξ_{merged} (17), $\{\tilde{\mathbf{B}}\}^{K}$ and ξ_{reduced} (18), as described in Section 2.2.4. However, MSRSD-USRLD differs from extended QRLPSA in that instead of summing the metrics from $\{\tilde{\mathbf{B}}\}_{\mathrm{QR}}^{m}$ and $\{\tilde{\mathbf{B}}\}_{\mathrm{QL}}^{m}$, the detection metric for the merged candidate label vectors are obtained by evaluating ML metric $\mathcal{A}$, given in Equation (4), for each candidate symbol vector pair in ξ_{merged}. The K candidate label vectors with the lowest merged detection metrics are again used for constructing $\{\tilde{\mathbf{B}}\}^{K}$ and ξ_{reduced}.

In Stage 3 of MSRSD-USTLD, N_{Tx} reduced sets of candidate symbol vector pairs, ξ_j^*, $j \in [1 : N_{\mathrm{Tx}}]$ are defined as the 'union sets'. The final estimate of the transmitted information is obtained by performing an ML search through the union sets as described by

$$\langle \tilde{\mathbf{x}}_1, \tilde{\mathbf{x}}_2 \rangle = \underset{\substack{\langle \hat{x}_{j_1}, \hat{x}_{j_2} \rangle \in \xi_j^* \\ j \in [1 : N_{\mathrm{Tx}}]}}{\arg\min} \mathcal{A}(\hat{\mathbf{x}}_1, \hat{\mathbf{x}}_2). \tag{20}$$

To generate the union sets, it is first necessary to perform preprocessing and generate a lookup table of M reduced constellation sets, ξ_i^{λ}. ξ_i^{λ} represents the λ most likely symbol vector pairs to be detected for transmitted information label i, where $1 < \lambda \leq M$. The metric chosen to determine which symbol pairs should be selected to build the reduced constellation sets is the product ED, as it is shown by Samra et al[10] and Xu et al[2] that USTLD mappers are designed to maximise the minimum product ED between labels across both constellation mappers. The product ED between the labels a and b is defined by

$$\prod d(a,b) = d_1(a,b) d_2(a,b), \tag{21}$$

where

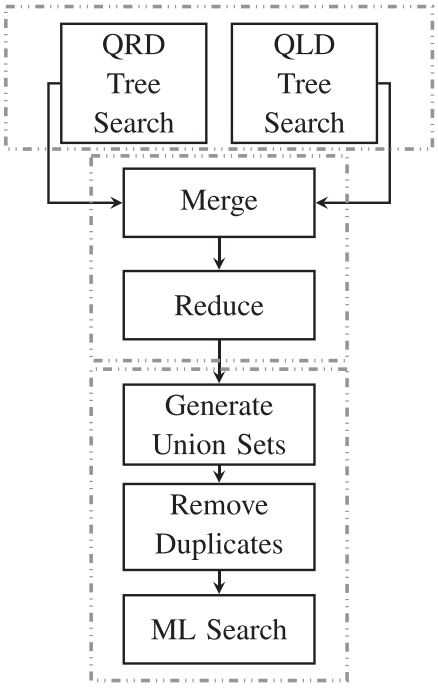

FIGURE 5 Block diagram of Multiple Stage Reduced Set Detection for USTLD (MSRSD-USTLD). QLD, QL decomposition; QRD, QR decomposition

$$d_t(a,b) = |\Omega_t(a) - \Omega_t(b)|^2;\ t \in [1:2] \tag{22}$$

is the squared ED between the symbols represented by labels a and b as a result of each mapper Ω_1 and Ω_2. To construct ξ_i^λ for label i, $i \in [0:M-1]$, the algorithm given in Table 1 is implemented.

Given the existence of the reduced constellation sets, the union set is constructed based on the output set of candidate label vectors from Stage 2 of MSRSD-USTLD, $\{\tilde{\mathbf{B}}\}^K = \left\{\tilde{\mathbf{B}}^{(1)}, \tilde{\mathbf{B}}^{(2)}, ..., \tilde{\mathbf{B}}^{(K)}\right\}$. Each candidate label vector is described by $\tilde{\mathbf{B}}^{(j)} = \left[\tilde{B}_1^{(i)} \ldots \tilde{B}_{N_{\mathrm{Tx}}}^{(j)}\right]^{\mathrm{T}}; j \in [1:K]$. Thus, the union set for transmitted label B_k, $k \in [1:N_{\mathrm{Tx}}]$ is defined as

$$\xi_k^* = \xi_{B_k^{(1)}}^\lambda \cup \xi_{B_k^{(2)}}^\lambda \cup \ldots \cup \xi_{B_k^{(K)}}^\lambda = \bigcup_{j \in [1:K]} \xi_{B_k^{(j)}}^\lambda. \tag{23}$$

The union set may be optimised by removing any duplicate entries in the set. As such, the cardinality of each union set is in the range $\lambda \le \left|\xi_j^*\right| \le K\lambda$.

It is noted that the search described in Equation (20) has worst-case ML search space $K\lambda^{N_{\mathrm{Tx}}}$, which incurs much higher complexity than the LCDAs discussed in Sections 2.2.1 to 2.2.4. However, by selecting a suitably small value for K and an appropriate λ, it is possible to ensure that $K\lambda^{N_{\mathrm{Tx}}} \ll M^{N_{\mathrm{Tx}}}$, thereby allowing significant complexity reduction compared to MLD. In this way, MSRSD-USTLD defines three adjustable parameters m, K, and λ, the values for which present a trade-off between detection accuracy and complexity. By comparison, the QRD-m[18] and QRLPSA[19] have only one degree of freedom (m), and the extended QRLPSA[20] has two (m and K).

A final optimisation to reduce the complexity of MSRSD-USTLD is to retain the m^2 ML metrics computed in Stage 2 of detection and reuse them in Stage 3 if any of the same candidate symbol vector pairs arise. Since $\left\langle \Omega_1\left(\{\tilde{\mathbf{B}}\}^K\right), \Omega_2(\{\tilde{\mathbf{B}}\}^K)\right\rangle \subset \xi_{\mathrm{merged}}$ and $\left\langle \Omega_1(\{\tilde{B}_j\}^K), \Omega_2(\{\tilde{B}_j\}^K)\right\rangle \subset \xi_j^*; j \in [1:N_{\mathrm{Tx}}]$, the maximum number of ML metrics computed during the third detection stage is reduced to $K(\lambda-1)^{N_{\mathrm{Tx}}}$.

3 | PERFORMANCE ANALYSIS

3.1 | ABEP for HR-USTLD

An approach to analysing the ABEP for a $2\times N_{\mathrm{Rx}}$ MIMO system in both fast-fading and quasi-static Rayleigh fading conditions is given by Xu et al.[2] This paper follows the same approach and extends it to the more general case of an $N_{\mathrm{Tx}} \times N_{\mathrm{Rx}}$ HR-USTLD system. An important assumption made at the start of the analysis by Xu et al[2] is that at high SNR, only one of the transmitted symbol pairs is incorrectly detected. This assumption is reasonable, as the the system is expected to have high link reliability at high SNRs. Therefore, the same assumption is also used when analysing the performance of HR-USTLD in this paper. Given this assumption, the bound of the ABEP for HR-USTLD is defined as[2]

TABLE 1 Algorithm for generating lookup table entries of $\xi_i^\lambda, i \in [1:M]$

Step 1:	Compute the product distances
	$\prod d(i,\hat{i}), \hat{i} \in [0:M-1]$ and store these as the set $\{\prod d\}^M$.
Step 2:	Sort $\{\prod d\}^M$ in ascending order.
Step 3:	Construct $\{\hat{i}\}^\lambda$ by storing the first λ candidate labels, $\hat{i}$, from the sorted list
	$\{\prod d\}^M$. The first label should always correspond to the case of
	$\prod d(i,\hat{i}) = 0$, which occurs when $i = \hat{i}$.
Step 4:	Construct the reduced constellation set ξ_i^λ by mapping the candidate label set $\{\hat{i}\}^\lambda$
	using the USTLD mappers, as described by
	$\xi_i^\lambda = \left\langle \Omega_1(\{\hat{i}\}^\lambda), \Omega_2(\{\hat{i}\}^\lambda)\right\rangle$.

Abbreviation: USTLD, uncoded space-time labelling diversity

$$P_e(\gamma) \leq \frac{1}{Mlog_2M} \sum_{i=0}^{M-1} \sum_{\substack{j=0 \\ j \neq i}}^{M-1} \delta(i,j) P\left(\mathbf{X} \rightarrow \tilde{\mathbf{X}}\right), \tag{24}$$

where $\delta(i,j)$ is the number of bit errors between the labels i and j, and $P\left(\mathbf{X} \rightarrow \tilde{\mathbf{X}}\right)$ is the pairwise error probability (PEP) of an erroneous detection of matrix $\mathbf{X} = [\mathbf{x}_1\ \mathbf{x}_2]$ to estimated matrix $\tilde{\mathbf{X}} = [\tilde{\mathbf{x}}_1\ \tilde{\mathbf{x}}_2]$.

For the sake of notation, and without loss of generality, it is assumed that the incorrectly detected symbol pair is $\langle \tilde{x}_{a_1}, \tilde{x}_{a_2} \rangle$, $a \in [1 : N_{\mathrm{Tx}}]$. The corresponding transmitted symbol pair is denoted $\langle x_{a_1}, x_{a_2} \rangle$. Hence, the PEP $P\left(\mathbf{X} \rightarrow \tilde{\mathbf{X}}\right)$ may be equivalently written as $P(\langle x_{a_1}, x_{a_2} \rangle \rightarrow \langle \tilde{x}_{a_1}, \tilde{x}_{a_2} \rangle)$.

Given the assumption that only one symbol pair is incorrect, Xu et al[2] have shown that the conditional PEP may be expressed as

$$\begin{aligned} P\left(\mathbf{X} \rightarrow \tilde{\mathbf{X}} | \, \mathbf{H}_1, \mathbf{H}_2\right) &= P(\langle x_{a_1}, x_{a_2} \rangle \rightarrow \langle \tilde{x}_{a_1}, \tilde{x}_{a_2} \rangle | \, \mathbf{H}_1, \mathbf{H}_2) \\ &= P\left(\sum_{k=1}^{2} \| \mathbf{y}_t - \sqrt{\frac{\gamma}{N_{\mathrm{Tx}}}} \mathbf{H}_t \tilde{\mathbf{x}}_t \|^2 < \sum_{k=1}^{2} \| \mathbf{n}_t \|^2 \right) \\ &= \mathcal{Q}\left(\sqrt{\phi_1 + \phi_2} \right), \end{aligned} \tag{25}$$

where $\mathcal{Q}(x) = \frac{1}{\pi} \int_0^{0.5\pi} \exp\left(0.5(x \mathrm{csc} y)^2\right) \mathrm{d}y$ is the Gaussian Q-function[28] and the cosecant is defined as $\mathrm{csc}(x) = \frac{1}{\sin(x)}$. In Equation (25), ϕ_1 and ϕ_2 are central chi-squared random variables which each have $2N_{\mathrm{Rx}}$ degrees of freedom.[2] The underlying Gaussian random variables that form ϕ_1 have zero mean and variance $\frac{\gamma}{4N_{\mathrm{Tx}}} |x_{a_1} - \tilde{x}_{a_1}|^2$. Similarly, the Gaussian random variables that form ϕ_2 have zero mean and variance $\frac{\gamma}{4N_{\mathrm{Tx}}} |x_{a_2} - \tilde{x}_{a_2}|^2$. The derivations for the variance of these random variables can be found in the work by Xu et al.[2]

As shown by Xu et al,[2] the unconditional PEP is found by integrating the conditional PEP, given by Equation (25), over the probability density functions of ϕ_1 and ϕ_2 and applying a trapezoidal approximation. This produces the result:

$$P\left(\mathbf{X} \rightarrow \tilde{\mathbf{X}}\right) \approx \frac{1}{4n} \prod_{t=1}^{2} \mathcal{M}_t\left(\frac{1}{2}\right) + \frac{1}{2n} \sum_{m=1}^{n-1} \prod_{t=1}^{2} \mathcal{M}_t\left(\frac{1}{2} \mathrm{csc}^2\left(\frac{m\pi}{2n}\right)\right), \tag{26}$$

where $\mathcal{M}_1(s)$ and $\mathcal{M}_2(s)$ are the respective moment generating functions (MGFs) of ϕ_1 and ϕ_2 under the assumption of N_{Rx} independent and identically distributed (i.i.d.) Rayleigh fading channels, and n is an arbitrarily large integer value that allows the summation to approximate an integral. Xu et al[2] have shown that the MGF for the specific case of $N_{\mathrm{Tx}} = 2$ is defined in terms of the variance of the Gaussian random variables that underlie ϕ_1 and ϕ_2. For the high-rate USTLD system described in this paper, the derivation provided by Xu et al[2] is generalised to describe a system of any arbitrary N_{Tx} transmit antennas. Expressing the resultant MGF in terms of the squared ED between labels, given in Equation (22), yields

$$\mathcal{M}_t(s) = \left(1 + \frac{\gamma}{2N_{\mathrm{Tx}}} d_t s\right)^{-N_{\mathrm{Rx}}}; \ t \in [1:2]. \tag{27}$$

Thus, the overall ABEP for an $N_{\mathrm{Tx}} \times N_{\mathrm{Rx}}$ HR-USTLD system in i.i.d. Rayleigh fading channels is obtained by substituting Equation (26) in Equation (24). The resulting expression is

$$P_e(\gamma) \leq \frac{1}{2nMlog_2M} \sum_{i=0}^{M-1} \sum_{\substack{j=0 \\ j \neq i}}^{M-1} \delta(i,j) \left[\frac{1}{2} \prod_{t=1}^{2} \mathcal{M}_t\left(\frac{1}{2}\right) + \sum_{m=1}^{n-1} \prod_{t=1}^{2} \mathcal{M}_t\left(\frac{1}{2} \mathrm{csc}^2\left(\frac{m\pi}{2n}\right)\right) \right]. \tag{28}$$

3.2 | Analytical evaluation of algorithmic complexity

When reviewing literature, it is found that the authors of the existing LCDAs discussed in Section 2.2 analyse complexity using different metrics.[18-20] In table I of the paper by Kim et al,[18] QRD-m is compared to MLD in terms of complex

additions, subtractions and multiplications, as well as real multiplications. Radosalvjevic et al[19] implement the QRLPSA on a field programmable gate array and evaluate its performance in terms of the number of arithmetic units used and the search latencies experienced in the hardware implementation. Finally, Peer et al[20] analyse the complexity of the extended QRLPSA in terms of the number of expanded nodes during the detection search. To fairly analyse and compare the LCDAs investigated in this work, a unified means of evaluating complexity is considered: the effective number of real mathematical operations performed during the detection process, which is denoted by the symbol Ψ. Real operations were also used by Pillay and Xu[4] in their complexity analysis of USTLD systems with media-based modulation. Complex addition, or subtraction, is considered to have two effective real operations and complex multiplication is considered to have six effective real operations. Vector norms are said to consist of $4|\mathbf{V}|-1$ operations, where $|\mathbf{V}|$ is the length of the vector.

According to Peer et al,[20] the complexity of decomposing matrix $\boldsymbol{H}$ by either QRD or QLD is negligible compared to the complexity of searching and is thus neglected.

The preprocessing and ordering of $\boldsymbol{H}$ incurs a complexity of $8N_{\mathrm{Tx}}N_{\mathrm{Rx}}-N_{\mathrm{Tx}}$ operations.

A summary of the complexity of each detection scheme is given in terms of the number of expanded nodes during the detection search in Table 2. Table 3 presents a similar summary in terms of the number of effective real operations, Ψ. Derivations for the expressions in Table 3 are provided in Appendix A1. Note that for MSRSD-USTLD, the complexity cannot be exactly determined (see Appendix A1, Section A.0.4). Thus, the expression given in the last row of Table 3 is for the upper bound of the complexity of MSRSD-USTLD.

4 | RESULTS AND DISCUSSION

Monte Carlo simulations were used to produce all the results presented in this section. In the first set of results, the analytical expression for the ABEP (28), which was derived in Section 3.1, is verified. As shown in Figure 6, simulation

TABLE 2 Complexity comparison of LCDAs in terms of number of candidate label vectors

LCDA	No. of candidate label vectors (nodes)
MLD	$M^{N_{\mathrm{Tx}}}$
QRD	MN_{Tx}
QRD-m[18]	$M+mM(N_{\mathrm{Tx}}-1)$
QRLPSA[19]	$2M+mM(N_{\mathrm{Tx}}-2)$
Extended QRLPSA[20]	$2M+mM(N_{\mathrm{Tx}}-2)+K\left\lfloor\frac{N_{\mathrm{Tx}}}{2}\right\rfloor$
MSRSD-USTLD	$2M+mM(N_{\mathrm{Tx}}-2)+m^2+K(\lambda-1)^{N_{\mathrm{Tx}}}$

Abbreviations: LCDA, low-complexity detection algorithm; MLD, maximum-likelihood detection; MSRSD-USTLD, multiple stage reduced set detection for uncoded space-time labelling diversity; QRD, QR decomposition; QRLPSA, QR-QL parallel searching algorithm.

TABLE 3 Complexity comparison of LCDAs in terms of effective real operations

LCDA	Number of effective real operations (Ψ)
MLD	$M^{N_{\mathrm{Tx}}}(16N_{\mathrm{Tx}}N_{\mathrm{Rx}}+8N_{\mathrm{Rx}}-1)$
QRD	$16N_{\mathrm{Rx}}^2-4N_{\mathrm{Rx}}+M\left(8N_{\mathrm{Tx}}^2+15N_{\mathrm{Tx}}\right)$
QRD-m[18]	$16N_{\mathrm{Rx}}^2-4N_{\mathrm{Rx}}+M\left(23+m\left(8N_{\mathrm{Tx}}^2+15N_{\mathrm{Tx}}-23\right)\right)$
QRLPSA[19]	$\begin{cases}32N_{\mathrm{Rx}}^2-8N_{\mathrm{Rx}}+M\left(46+m\left(4N_{\mathrm{Tx}}^2+15N_{\mathrm{Tx}}-46\right)\right); \text{even } N_{\mathrm{Tx}}\\ 32N_{\mathrm{Rx}}^2-8N_{\mathrm{Rx}}+M\left(46+m\left(4N_{\mathrm{Tx}}^2+15N_{\mathrm{Tx}}-42\right)\right); \text{odd } N_{\mathrm{Tx}}\end{cases}$
Extended QRLPSA[20]	$\begin{cases}\Psi_{\mathrm{QRLPSA,\,even}\ N_{\mathrm{Tx}}}+m^2+K\left(6N_{\mathrm{Tx}}^2+\frac{15}{2}N_{\mathrm{Tx}}\right); \text{even } N_{\mathrm{Tx}}\\ \Psi_{\mathrm{QRLPSA,\,odd}N_{\mathrm{Tx}}}+m^2+K\left(6N_{\mathrm{Tx}}^2+\frac{23}{2}N_{\mathrm{Tx}}+\frac{11}{2}\right); \text{odd } N_{\mathrm{Tx}}\end{cases}$
MSRSD-USTLD	$\Psi_{\mathrm{QRLPSA}}+\left(m^2+K(\lambda-1)^{N_{\mathrm{Tx}}}\right)(16N_{\mathrm{Tx}}N_{\mathrm{Rx}}+8N_{\mathrm{Rx}}-1)$

Abbreviations: LCDA, low-complexity detection algorithm; MLD, maximum-likelihood detection; MSRSD-USTLD, multiple stage reduced set detection for uncoded space-time labelling diversity; QRD, QR decomposition; QRLPSA, QR-QL parallel searching algorithm.

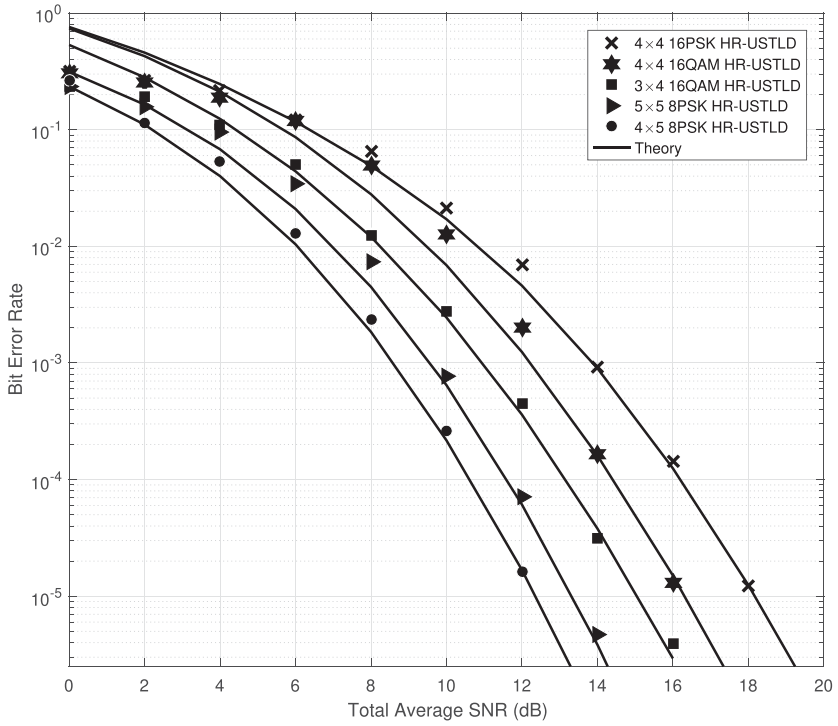

FIGURE 6 Analytical average bit error probability (ABEP) converging to simulated results using maximum-likelihood (ML) detection. HR-USTLD, high-rate uncoded space-time labelling diversity

results based on MLD converge to the theoretical ABEP in the high SNR region. Results are presented for various antenna array sizes, modulation orders, and for both QAM and PSK modulation.

From the results in Figure 6, it is further observed that there is a difference of 1 dB between the 4×5 and 5×5 8PSK HR-USTLD systems at a BER of 10^{-6}. The same observation is made when comparing the 3×4 and 4×4 16QAM HR-USTLD systems. These observations indicate that increasing the number of transmit antennas in the HR-USTLD system results in higher data rates at the cost of poorer BER performance. This trade-off between data rate and error performance is typical of MIMO systems that achieve spatial multiplexing, such as the V-BLAST architecture.[24] The reason for the degradation in error performance can be explained mathematically. Considering the equation for the MGF given in Equation (27), when N_{Tx} is increased, the MGF increases as well. Thus, the result for the ABEP calculated using Equation (28) will increase, indicating inferior error performance. The intuitive interpretation of this (based on the system model defined in Section 2.1) is that splitting the total average SNR across more transmit antennas results in less power being allocated to each antenna. Thus, the energy of each of the transmitted symbols at the receiver is reduced, increasing the likelihood of an incorrect detection.

The next set of results compares the performance of HR-USTLD and similar schemes of equal data rate. The results presented in Figure 8 compare the theoretical performance of six systems which achieve a data rate of six bits/s/Hz: (i) a conventional 3×4 4QAM MIMO system, (ii) a conventional 1×4 64QAM single-input, multiple-output (SIMO) system, (iii) a 2×4 64QAM Alamouti space-time block coded system,[9] (iv) a 2×4 64QAM USTLD system,[2] (v) a 3×4 64QAM USTLD system with three labelling diversity mappers,[11] and (vi) a 3×4 16QAM HR-USTLD system. It is highlighted that the 'conventional' SIMO and MIMO systems considered utilise a single time slot to transmit information[6] and that the USTLD system with three labelling diversity mappers utilises three time slots to transmit information.[11] The mappers used for the three mapper USTLD system are constructed by following the design rules presented in Section 4 of the work by Ayanda et al.[11] The results in Figure 7A show that by using a lower order modulation and more transmit antennas, the 3×4 16QAM HR-USTLD system outperforms the existing 2×4 64QAM USTLD system by approximately 4 dB in the high SNR region.The gradient of the curves also confirm that HR-USTLD achieves similar diversity to the original USTLD model. This may be quantified in terms of the diversity order, Γ, which is defined as[29]

$$\Gamma = -\lim_{\gamma \to \infty} \frac{log P_e(\gamma)}{log\, \gamma}. \tag{29}$$

By using Equation (29) to determine the diversity order of each of the systems presented in Figure 7A, the results given in Figure 7B are obtained. The values for $\Gamma_{\mathrm{Alamouti}}$ and $\Gamma_{\mathrm{USTLD\ (3\ Mappers)}}$ match those that have been reported in

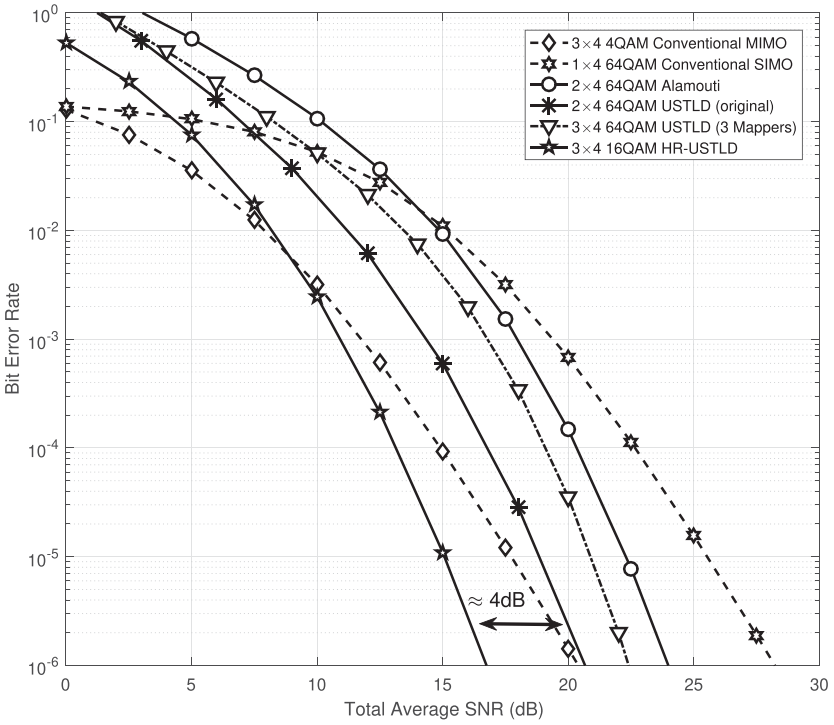

(A) Bit Error Rate Comparison

Transmission Scheme	Diversity Order (Γ)
Conventional MIMO[6]	N_{Rx}
Conventional SIMO[6]	N_{Rx}
Alamouti[9]	$2N_{\mathrm{Rx}}$
USTLD (original)[2]	$2N_{\mathrm{Rx}}$
USTLD (3 Mappers)[11]	$3N_{\mathrm{Rx}}$
HR-USTLD	$2N_{\mathrm{Rx}}$

(B) Diversity Order Comparison

FIGURE 7 Error performance comparison of uncoded systems with equal data rate. HR-USTLD, high-rate USTLD; MIMO, multiple-input, multiple-output; SIMO, single-input, multiple-output; USTLD, uncoded space-time labelling diversity detection

literature.[9,11] The values obtained for $\Gamma_{\mathrm{USTLD\ (original)}}$, $\Gamma_{\mathrm{USTLD\ (3\ Mappers)}}$ and $\Gamma_{\mathrm{HR\text{-}USTLD}}$ indicate that the diversity order of USTLD systems is a product of the number of time slots over which the same information is transmitted and the number of receive antennas. Stated differently, the diversity order represents the total number of independent copies of the same information codeword that are available at the receiver when performing detection. It is interesting to note that the number of labelling diversity mappers in the system does not directly influence the diversity order. This is shown most clearly by the result that $\Gamma_{\mathrm{Alamouti}} = \Gamma_{\mathrm{USTLD\ (original)}} = 2N_{\mathrm{Rx}}$. Qualitative analysis of the results presented in other works that apply labelling diversity to systems that utilise only one transmission time slot, such as those studied by Naidoo,[30] also indicate that diversity order is unaffected by labelling diversity.

This leads to an interesting deduction which was not reported in the original work on USTLD systems[2]—the inclusion of labelling diversity in a MIMO system does not change the diversity order of the system. Rather, the BER performance improvement as a result of labelling diversity is qualitatively observed by a lateral shift of the high-SNR region of BER versus total average SNR curve (as shown in Figure 7A). These lateral shifts of the BER versus total average SNR curve are generally typical of a coding gain;[6] however, labelling diversity achieves this benefit without introducing coding to the system.

A further observation that is drawn from the results in Figure 8 highlights the importance of mapper design for USTLD systems. In their work, Ayanda et al[11] compared their three mapper USTLD with a two mapper USTLD system based on the secondary mapper design by Xu et al[2] for a 64QAM USTLD system. It was since shown by Quazi and

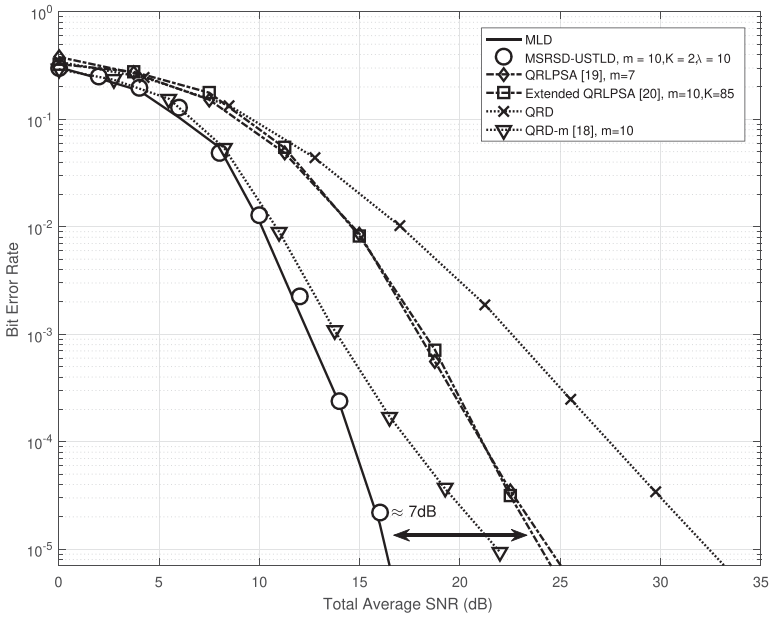

(A) Comparison of Accuracy

FIGURE 8 Comparison of LCDAs for 4 × 4 16QAM HR-USTLD. LCDA, low-complexity detection algorithm; MLD, maximum-likelihood detection; MSRSD-USTLD, multiple stage reduced set detection for uncoded space-time labelling diversity; QRD, QR decomposition; QRLPSA, QR-QL parallel searching algorithm

LCDA	No. of Candidate Label Vectors
QRD	64
QRD-m, $m = 10$	496
QRLPSA, $m = 7$	256
Extended QRLPSA, $m = 10, K = 85$	522
MSRSD-USTLD, $m = 10, K = 2, \lambda = 10$	13 574
MLD	65 536

(B) Comparison of Complexity - Candidate Label Vectors

LCDA	Ψ_{LCDA}	% Reduction in Ψ
QRD	3 372	99.98%
QRD-m, $m = 10$	27 132	99.86%
QRLPSA, $m = 7$	10 076	99.95%
Extended QRLPSA, $m = 10, K = 85$	24 630	99.87%
MSRSD-USTLD, $m = 10, K = 2, \lambda = 10$	3 808 534	79.75%
MLD	18 808 832	0%

(C) Comparison of Complexity - Effective Real Operations

Patel[3] that the secondary mapper design technique by Seddik et al[25] is better than that proposed by Xu et al for 64QAM modulation. The results in Figure 7A show that the 3×4 64QAM USTLD system with three mappers[11] performs worse than the original 2×4 64QAM two mapper USTLD system[2] (utilising the secondary mapper design proposed by Seddik et al) by approximately 2 dB. This emphasises that mapper design has a drastic influence on the error performance of USTLD systems. It may thus be inferred that the error performance of the HR-USTLD systems presented in this paper may be further improved in future works if better mapper designs are developed.

The final set of results in this paper investigates the performance of QRD-based LCDAs on HR-USTLD. Algorithms are compared in terms of accuracy and complexity to the benchmark case of MLD. Accuracy is observed graphically by the closeness of the BER curves to the MLD case, and complexity is compared by using the equations presented in Tables 2 and 3. Since the number of effective real operations gives a more realistic indication of performance, the

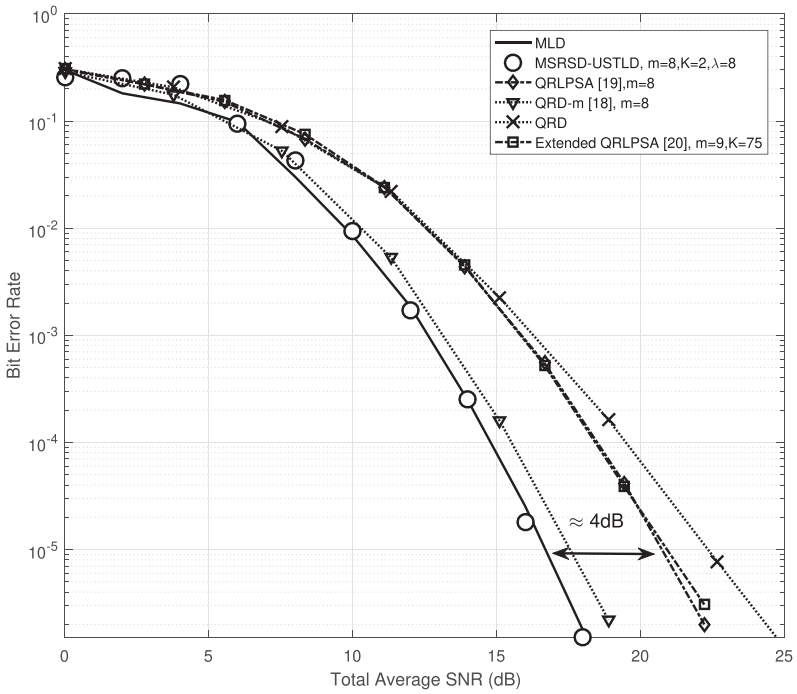

FIGURE 9 Comparison of low-complexity detection algorithms (LCDAs) for 4 × 5 16PSK HR-USTLD. LCDA, low-complexity detection algorithm; MLD, maximum-likelihood detection; MSRSD-USTLD, multiple stage reduced set detection for uncoded space-time labelling diversity; QRD, QR decomposition; QRLPSA, QR-QL parallel searching algorithm

(A) Comparison of Accuracy

LCDA	No. of Candidate Label Vectors
QRD	64
QRD-m, $m = 8$	400
QRLPSA, $m = 8$	288
Extended QRLPSA, $m = 9, K = 75$	470
MSRSD-USTLD, $m = 8, K = 2, \lambda = 8$	5 154
MLD	65 536

(B) Comparison of Complexity - Candidate Label Vectors

LCDA	Ψ_{LCDA}	% Reduction
QRD	3544	99.98%
QRD-m, $m = 8$	22 024	99.91%
QRLPSA, $m = 8$	11 636	99.95%
Extended QRLPSA, $m = 9, K = 75$	22 415	99.90%
MSRSD-USTLD, $m = 8, K = 2, \lambda = 8$	1 758 530	92.53%
MLD	23 527 424	0%

(C) Comparison of Complexity - Effective Real Operations

discussion focusses on this metric. It is also useful to define the percentage reduction in effective real operations for an LCDA, which is given by

$$\%\ \text{Reduction of}\ \Psi_{\text{LCDA}} = 1 - \frac{\Psi_{\text{LCDA}}}{\Psi_{\text{MLD}}}. \tag{30}$$

From the results presented in Figures 8 and 9, it is clear that existing QRD-based LCDAs are unsuitable for HR-USTLD systems. Despite reducing the number of effective real operations by over 99%, these schemes fail to capture the

system diversity and do not achieve detection accuracy comparable to MLD. By contrast, the proposed MSRSD-USTLD algorithm achieves near-ML accuracy. The results indicate that there is a significant complexity cost associated with this increase in accuracy, as expected, when comparing MSRSD-USTLD to existing QRD-based LCDAs. However, MSRSD-USTLD provides considerable complexity reduction when compared to the benchmark case of MLD. For high modulation orders, the achievable complexity reduction of MSRSD-USTLD may be approximated as $1-\left(\frac{\lambda-1}{M}\right)^{N_{\mathrm{Tx}}}$. For reasonable values such as $\lambda = 35$ and a $4 \times N_{\mathrm{Rx}}$ 64-ary QAM or PSK system, this results in complexity reduction of approximately $1-\left(\frac{34}{64}\right)^4 = 92.03\%$.

The final study in this paper presents the inherent trade-off between detection accuracy and complexity for the MSRSD-USTLD algorithm. As mentioned in Section 2.2.5, MSRSD-USTLD defines three parameters (m, K, and λ) that can be tuned to adjust the trade-off between detection accuracy and complexity. This study focusses on effect of the reduced constellation set size (λ), which is the additional variable introduced to the detection when compared to the Extended QRLPSA.[20] The expression for the complexity of MSRSD-USTLD presented in Table 3 also shows that, of the three adjustable parameters in the MSRSD-USTLD algorithm, λ has the greatest impact on complexity.

Figure 10 presents the results of this study for discrete values of λ, tested on a 4×4 16QAM HR-USTLD system at a total average SNR of 14 dB. The other parameters for performing MSRSD-USTLD on this system were $m = 10$ and $K = 2$. The results indicate that higher values of λ result in more accurate detection, as expected. When $\lambda = M$, the union set used in Stage 3 of the MSRSD-USTLD algorithm is the same as the MLD search set. In other words, the BER simulated for $\lambda = 16$ in Figure 10 is the same as the BER that would be obtained by implementing MLD and is the benchmark when comparing the detection accuracy of the algorithm. It is observed that when $\lambda \geq 12$, there is minimal change in the simulated BER of the system. Hence, choosing λ in this range achieves optimal detection accuracy for the USTLD system considered. Figure 10 also shows that the maximum complexity of MSRSD-USTLD increases as λ increases. It is observed that for $\lambda = 14$, the complexity of MSRSD-USTLD is approximately the same as MLD. For greater values of λ, MSRSD-USTLD is found to incur a higher complexity than MLD. This is expected, as when $\lambda \approx M$, the complexity of Stage 3 of the MSRSD-USTLD algorithm is comparable to MLD. However, when summing the complexity of all three stages of MSRSD-USTLD, a higher complexity than MLD is obtained. It may thus be concluded that for the system presented, choosing $\lambda = 12$ allows for near-optimal detection accuracy to be achieved at approximately 50% of the complexity of MLD.

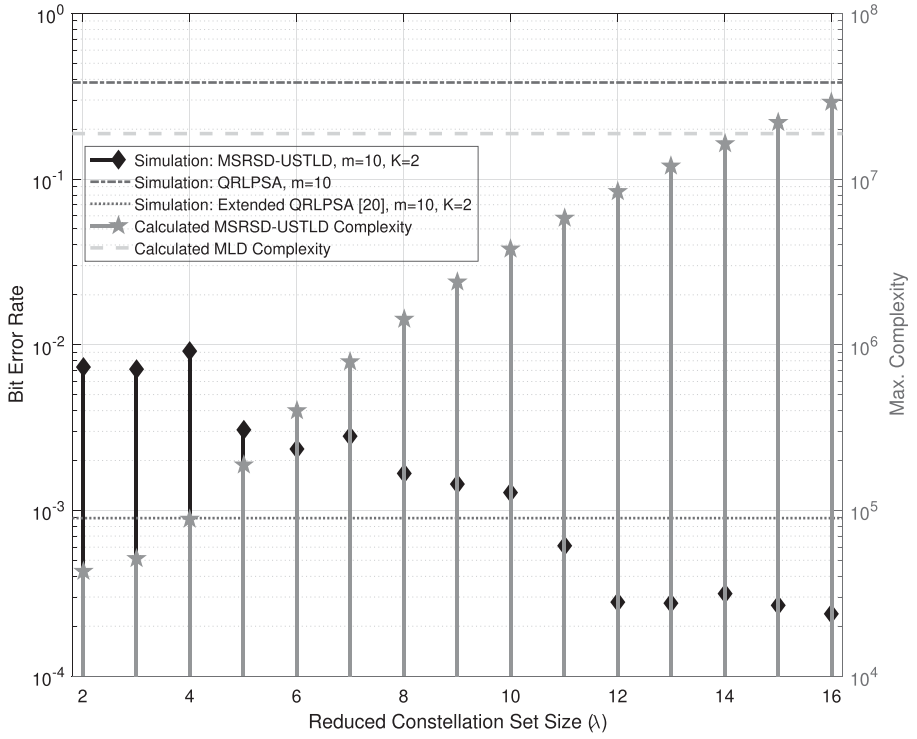

FIGURE 10 Demonstrating the trade-off between accuracy and complexity of MSRSD-USTLD. MLD, maximum-likelihood detection; MSRSD-USTLD, multiple stage reduced set detection for uncoded space-time labelling diversity; QRLPSA, QR-QL parallel searching algorithm

5 | CONCLUSION

In this paper, USTLD was extended to a more general case of any N_{Tx} transmit antennas. The motivation behind such an extension is that increasing N_{Tx} allows for higher data rates to be achieved at lower modulation orders, which results in better system error performance. Results confirm this and show a 4 dB performance improvement between HR-USTLD and existing USTLD systems for a six bits/s/Hz data rate. In addition to defining the HR-USTLD system model, this paper derives an analytical expression for the upper bound of the ABEP, which is verified against simulated results.

To combat the exponential increase in computational complexity associated with systems with multiple transmit antennas, a new LCDA designed specifically for the HR-USTLD system is presented (MSRSD-USTLD). It is shown that MSRSD-USTLD is capable of achieving near-ML detection accuracy. From the systems investigated, the worst-case complexity of MSRSD-USTLD is shown to still achieve 79.75% complexity reduction when compared to MLD in a 4×4 16QAM HR-USTLD system and 92.53% reduction in a 4×5 16PSK HR-USTLD system. Results have been presented to demonstrate the trade-off between detection accuracy and complexity for MSRSD-USTLD. It is noted that although the MSRSD-USTLD algorithm proposed has been developed using QRD-based LCDAs in its initial stages, this is not a strict constraint. As such, future works may investigate the application of other existing LCDAs in the initial stages of MSRSD-USTLD. Future works may also consider developing analytical expressions for the error performance of HR-USTLD systems when sub-optimal LCDAs are applied to them.

ORCID

Sulaiman Saleem Patel https://orcid.org/0000-0003-3557-3645
Tahmid Quazi https://orcid.org/0000-0002-1288-4224
Hongjun Xu https://orcid.org/0000-0002-5768-1965

REFERENCES

1. Simon MK, Alouini M-S. *Digital Communication over Fading A Unified Approach to Performance Analysis*. New York (USA): John Wiley & Sons Inc.; 2000.
2. Xu H, Govindasamy K, Pillay N. Uncoded space-time labeling diversity. *IEEE Commun Lett*. 2016;20(8):1511-1514.
3. Quazi T, Patel SS. USTLD Mapper design for APSK constellation over satellite channels. *Trans Emerging Telecomm Tech*. 2019:e3586. https://doi.org/10.1002/ett.3586
4. Pillay N, Xu H. Uncoded space-time labeling diversity—application of media-based modulation with RF mirrors. *IEEE Commun Lett*. 2018;22(2):272-275.
5. Patel SS, Quazi T, Xu H. A genetic algorithm for uncoded space-time labelling diversity mapper design,; 2018:77-82. https://doi.org/10.1109/SiPS.2018.8598435
6. Goldsmith A. *Wireless Communications Cambridge*. (USA): Cambridge University Press; 2005.
7. Cormen TH, Leiserson CE, Rivest RL, Stein C. *Introduction to Algorithms Cambridge*. (USA): The MIT Press; 2009.
8. Fincke U, Pohst M. Improved methods for calculating vectors of short length in a lattice. *Math Comput*. 1985;44(170):463-471.
9. Alamouti SM. Simple transmit diversity technique for wireless communications. *IEEE J on Sel Areas in Commun*. 1998;16(8):1451-1458.
10. Samra H, Ding Z, Hahn P. Symbol mapping diversity design for multiple packet transmissions. *IEEE Trans Commun*. 2005;53(5):810-817.
11. Ayanda D, Xu H, Pillay N. Uncoded M-ary quadrature amplitude modulation space-time labeling diversity with three transmit antennas. *Int J Commun Syst*. 2018:e3818. https://doi.org/10.1002/dac.3818
12. Xu R, Lau FCM. Performance analysis for MIMO systems using zero forcing detector over fading channels. *IEE Proc Commun*. 2006;153(1):74-80.
13. Prasad S, Sur SN. Lattice reduction aided detection techniques for MIMO systems. *Int Research Jour of Eng and Tech*. 2016;3(3):1496-1502.
14. Jiang Y, Varanasi MK, Li J. Performance analysis of ZF and MMSE equalizers for MIMO systems: an in-depth study of the high SNR regime. *IEEE Trans Inf Theory*. 2011;57(4):2008-2026.
15. Neinavaie M, Derakhtian M. ML performance achieving algorithm with the zero-forcing complexity at high SNR regime. *IEEE Trans Wireless Commun*. 2016;15(7):4651-4659.
16. Hassibi B, Vikalo H. On the sphere-decoding algorithm I. Expected complexity. *IEEE Trans Signal Process*. 2005;53(8):2806-2818.
17. Vikalo H, Hassibi B. On the sphere-decoding algorithm II. Generalizations, second-order statistics, and applications to communications. *IEEE Trans Signal Process*. 2005;53(8):2819-2834.
18. Kim KJ, Yue J, Iltis RA, Gibson JD. A QRD-D/Kalman Filter-based detection and channel estimation algorithm for MIMO-OFDM systems. *IEEE Trans Wirel Commun*. 2005;4(2):710-721.
19. Radosavljevic P, Kim KJ, Shen H, Cavallaro JR. Parallel searching-based sphere detector for MIMO downlink OFDM systems. *IEEE Trans Signal Process*. 2012;60(6):3240-3252.

20. Peer N, Murin Y, Dabora R. Improved QRD-QLD algorithm for low complexity MIMO decoding. *IEEE Commun Lett*. 2014;18 (10):1703-1706.
21. Govindasamy K. Space-time labelling diversity and space-time block coded spatial modulation with labelling diversity. *Masters Thesis*: University of Kwa-Zulu Natal; 2015.
22. Govindasamy K, Xu H, Pillay N. Space-time block coded spatial modulation with labeling diversity. *Int J Commun Syst*. 2017;31(1): e3395. https://doi.org/10.1002/dac.3395
23. Haykin S, Moher M. *Communication Systems*. 5th ed: John Wiley & Sons Inc.; 2010.
24. Wolniansky PW, Foschini GJ, Golden GD, Valenzuela RA. V-BLAST: an architecture for realizing very high data rates over the rich-scattering wireless channel. In: Proc. 1998 URSI Int. Symp. on Sig., Syst. and Electronics; 1998; Pisa (Italy):1998. https://doi.org/10.1109/ISSSE.1998.738086
25. Seddik KG, Ibrahim AS, Liu KJR. Trans-modulation in wireless relay networks. *IEEE Commun Lett*. 2008;12(3):170-172.
26. Dai Y, Sun S, Lei Z. A Comparative study of QRD-M detection and sphere decoding for MIMO-OFDM systems. In: Proc. IEEE Int. Symp. Pers., Indoor and Mobile Radio Commun Syst.; 2005; Berlin (Germany):186-190.
27. Ming-jie Z. Performance analysis of a QR decomposition algorithm employing rearrangement of antenna layers on V-BLAST systems. *Int J Dig Content Tech and its App*. 2012;6(19):74-83. https://doi.org/10.4156/jdcta.vol6.issue19.10
28. Craig JW. A new, simple and exact result for calculating the probability of error for two-dimensional signal constellations. In: IEEE Military Commun. Conf. (MILCOM) McLean; 1991; VA (USA):571-575.
29. Zhang H, Dai H, Zhou Q, Hughes BL. On the diversity order of spatial multiplexing systems with transmit antenna selection: a geometrical approach. *IEEE Trans Inf Theory*. 2006;52(12):5297-5311.
30. Naidoo NR. *Enhanced Performance and Efficiency Schemes for Generalised Spatial Modulation*; University of Kwa-Zulu Natal; 2017.
31. Weisstein EW. Triangular Number (A Wolfram Web Resource). [Online Resource] http://mathworld.wolfram.com/TriangularNumber.html; 2017.

How to cite this article: Patel SS, Quazi T, Xu H. High-rate uncoded space-time labelling diversity with low-complexity detection. *Int J Commun Syst*. 2020;33:e4520. https://doi.org/10.1002/dac.4520

APPENDIX A: A DERIVATIONS OF COMPLEXITY IN TERMS OF EFFECTIVE REAL OPERATIONS

In the work of Pillay and Xu,[4] it is suggested that algorithmic complexity be measured in terms of real operations. This paper considers the same metric when determining the complexity of the detection schemes considered. When working with complex numbers, a single complex multiplication consists of four real multiplications and two real additions, equalling six effective real operations. Complex addition consists of two real additions and similarly for complex subtractions. The derivation of complexity in terms of this metric for the detection schemes given in Section 2.2 follows.

MLD derivation

MLD for HR-USTLD is done by evaluating the decision metric given in Equation (4) for each of the $M^{N_{\text{Tx}}}$ possible vector pairs $\langle \hat{\mathbf{x}}_1, \hat{\mathbf{x}}_2 \rangle$, where $\langle \hat{x}_{i_1}, \hat{x}_{i_2} \rangle \in \xi, i \in [1 : N_{\text{Tx}}]$. For a given vector $\hat{\mathbf{x}}_t, t \in [1 : 2]$, the following derives the complexity of calculating vector norm $\|\mathbf{z}_t - \mathbf{H}_t \hat{\mathbf{x}}_t\|^2$:

1 Matrix product $\mathbf{H}_t \hat{\mathbf{x}}_t$: $N_{\text{Tx}} N_{\text{Rx}}$ complex multiplications, $N_{\text{Rx}} N_{\text{Tx}} - N_{\text{Rx}}$ complex additions.
2 Vector subtraction $\mathbf{z}_t - \mathbf{H}_t \hat{\mathbf{x}}_t$: N_{Rx} complex subtractions.
3 Vector norm $\|\mathbf{z}_t - \mathbf{H}_t \hat{\mathbf{x}}_t\|^2$: $4N_{\text{Rx}} - 1$ real operations.

This gives a total of $8N_{\text{Tx}}N_{\text{Rx}} + 4N_{\text{Rx}} - 1$ effective real operations. It then follows that the complexity of MLD is given by

$$\begin{aligned} \Psi_{\text{MLD}} &= M^{N_{\text{Tx}}}(2(8N_{\text{Tx}}N_{\text{Rx}} + 4N_{\text{Rx}} - 1) + 1) \\ &= M^{N_{\text{Tx}}}(16N_{\text{Tx}}N_{\text{Rx}} + 8N_{\text{Rx}} - 1). \end{aligned} \tag{A1}$$

QRD, QRD-m, and QRLPSA derivations

For QRD, QRD-m, and QRLPSA, the derivations presented are for perfectly determined systems. This approach is identical when considering overdetermined systems if zero rows are discarded. Preprocessing by reordering $\boldsymbol{H}$ is not considered part of the algorithm, and the complexity of performing the actual decompositions (i.e. converting $\boldsymbol{H}$ to matrix product $\boldsymbol{QR}$ or matrix product $\boldsymbol{QL}$) is neglected, as per Peer et al.[20]

When considering any QRD-based detection schemes, the first step of detection after decomposing matrix $\boldsymbol{H}$ is to perform left-multiplication as shown in Equation (5). This matrix multiplication consists of $2N_{\text{Rx}}^2$ complex multiplications and $2N_{\text{Rx}}(N_{\text{Rx}} - 1)$ complex additions, giving a total complexity of $16N_{\text{Rx}}^2 - 4N_{\text{Rx}}$ effective real operations. The left-multiplication for a QLD-based system, which is necessary for the QRLPSA, is described by Equation (6) and incurs the same complexity as for QRD. Searching through the q-th layer of the QRD search tree during time slot t, as described by Equation (9), the complexity may be calculated as

1 Summation S_{1_t}: $q - 1$ complex multiplications, $q - 2$ complex additions.
2 Scalar subtraction $\alpha_{q_t} - r_{q,\,q_t}\hat{x}_t - S_{1_t}$: 1 complex multiplication, 2 complex subtractions.
3 ED $\left|\alpha_{q_t} - r_{q,q_t}\hat{x}_t - S_{1_t}\right|^2$: 3 real operations.

Thus, the complexity of searching through the q-th layer of the QRD search tree has $8q + 3$ effective real operations. Summing this result across both time slots yields:

$$\Psi_{\text{layer}}(q) = 2(8q + 3) + 1 = 16q + 7. \tag{A2}$$

The complexity for searching though the QRD tree is found by summing the result of (A2) through all N_{Tx} layers of the QRD search tree and testing M candidate symbol pairs per layer. Using the identity given by Weisstein,[31] $\sum_{k=1}^{A} k = \frac{A}{2}(A + 1)$, the result is

$$\begin{aligned}\Psi_{\text{QRD}} &= 16N_{\text{Rx}}^2 - 4N_{\text{Rx}} + M\sum_{q=1}^{N_{\text{Tx}}}\Psi_{\text{layer}}(q)\\ &= 16N_{\text{Rx}}^2 - 4N_{\text{Rx}} + M\left(8N_{\text{Tx}}^2 + 15N_{\text{Tx}}\right),\end{aligned} \tag{A3}$$

where the first two terms are as a result of the left-multiplication as explained previously. The same result is obtained for a QLD search tree.

For QRD-m, Equation (A3) is adjusted to cater for the m search paths considered from the second search layer onwards, yielding:

$$\begin{aligned}\Psi_{\text{QRD-m}} &= 16N_{\text{Rx}}^2 - 4N_{\text{Rx}} + M\Psi_{\text{layer}}(1) + mM\sum_{q=2}^{N_{\text{Tx}}}\Psi_{\text{layer}}(q)\\ &= 16N_{\text{Rx}}^2 - 4N_{\text{Rx}} + 23M + mM\left(8N_{\text{Tx}}^2 + 15N_{\text{Tx}} - 23\right).\end{aligned} \tag{A4}$$

For parallel searching, it is sufficient to consider only the complexity of the QRD search tree and double the result to take the QLD search tree into account. While traversing the search tree, the best m paths of the search tree are considered, and M nodes are expanded at each layer, for each path. Only $\left\lfloor \frac{N_{\text{Tx}}}{2} \right\rfloor$ layers of the QRD and QLD search trees may be evaluated in parallel, and for odd N_{Tx}, the $\left\lceil \frac{N_{\text{Tx}}}{2} \right\rceil$-th layer is evaluated after parallel searching.

Thus, the complexity of QRLPSA may be expressed as

$$\begin{aligned}\Psi_{\text{QRLPSA}} &= \left(\left\lceil \frac{N_{\text{Tx}}}{2} \right\rceil - \left\lfloor \frac{N_{\text{Tx}}}{2} \right\rfloor\right)\Psi_{\text{layer}}\left(\left\lceil \frac{N_{\text{Tx}}}{2} \right\rceil\right)\\ &\quad + 2\left(16N_{\text{Rx}}^2 - 4N_{\text{Rx}} + M\Psi_{\text{layer}}(1) + mM\sum_{q=2}^{\left\lfloor \frac{N_{\text{Tx}}}{2} \right\rfloor}\Psi_{\text{layer}}(q)\right).\end{aligned} \tag{A5}$$

Solving for the cases of even and odd N_{Tx} respectively yields:

$$\begin{aligned}\Psi_{\text{QRLPSA, even } N_{\text{Tx}}} &= 32N_{\text{Rx}}^2 - 8N_{\text{Rx}} + 46M + mM(4N_{\text{Tx}}^2 + 15N_{\text{Tx}} - 46).\\ \Psi_{\text{QRLPSA, odd } N_{\text{Tx}}} &= 32N_{\text{Rx}}^2 - 8N_{\text{Rx}} + 46\,M + mM(4N_{\text{Tx}}^2 + 15N_{\text{Tx}} - 42).\end{aligned} \tag{A6}$$

Extended QRLPSA derivation

For the extended QRLPSA, the first stage is to perform parallel searching, and thus, it incurs the complexity described by Equations (A5)–(A7). During the second stage, there are only m^2 real additions as a result of summing the metrics of the partial candidate label vectors during merging. Sorting and reducing to the set of K merged vectors incurs minimal complexity and is neglected. Finally, the complexity of the third stage is found by evaluating Equation (A2) for the latter $\left\lceil \frac{N_{\text{Tx}}}{2} \right\rceil$ layers of the QRD search tree and expanding K nodes per layer. Thus, the complexity of extended QRLPSA is

$$\begin{aligned}\Psi_{\text{Extended QRLPSA}} &= \Psi_{\text{QRLPSA}} + m^2 + K\sum_{q=\left\lceil \frac{N_{\text{Tx}}}{2} \right\rceil}^{N_{\text{Tx}}}\Psi_{\text{layer}}(q)\\ &= \Psi_{\text{QRLPSA}} + m^2 + K\left(\sum_{p=1}^{N_{\text{Tx}}}\Psi_{\text{layer}}(p) - \sum_{q=1}^{\left\lfloor \frac{N_{\text{Tx}}}{2} \right\rfloor}\Psi_{\text{layer}}(q)\right).\end{aligned} \tag{A8}$$

For even and odd N_{Tx}, the summation term reduces to $K\left(6N_{\text{Tx}}^2 + \frac{15}{2}N_{\text{Tx}}\right)$ and $K\left(6N_{\text{Tx}}^2 + \frac{23}{2}N_{\text{Tx}} + \frac{11}{2}\right)$, respectively.

MSRSD-USTLD derivation

Similarly to extended QRLPSA, the first stage of MSRSD-USTLD is to perform parallel searching, the complexity of which is given in Equations (A5)–(A7). Stages 2 and 3 both evaluate the MLD detection metric $\mathcal{A}$, which has been

defined in Equation (4), through ξ_{merged} and ξ_{reduced}, respectively. Complexity for each of these stages may be found by using the result from Equation (A1) for the complexity of the ML metric and multiplying by the cardinality of the respective search set. For Stage 2, $\left|\xi_{\text{merged}}\right| = m^2$, and thus, the complexity is

$$\Psi_{\text{MSRSD-USTLD, Stage 2}} = m^2(16N_{\text{Tx}}N_{\text{Rx}} + 8N_{\text{Rx}} - 1). \tag{A9}$$

For Stage 3, due to the optimisations outlined in Section 2.2.5, the size of the search space $|\xi_{\text{reduced}}|$ cannot be exactly determined. The maximum size of the reduced set search space is given by $|\xi_{\text{reduced}}|_{\max} = K(\lambda-1)^{N_{\text{Tx}}}$. Thus, the resulting upper bound on the Stage 3 complexity is

$$\Psi_{\text{MSRSD-USTLD, Stage 3}} \leq K(\lambda-1)^{N_{\text{Tx}}}(16N_{\text{Tx}}N_{\text{Rx}} + 8N_{\text{Rx}} - 1). \tag{A10}$$

Finally, the complexity of MSRSD-USTLD is given by

$$\Psi_{\text{MSRSD-USTLD}} \leq \Psi_{\text{QRLPSA}} + \Psi_{\text{MSRSD-USTLD, Stage 2}} + \Psi_{\text{MSRSD-USTLD, Stage 3}}. \tag{A11}$$

Substituting Equations (A5), (A9), and (A10) into Equation (A11) produces the expression given in Table 3.

The complexity of Stages 2 and 3 of MSRSD-USTLD is typically much larger than the complexity of Stage 1. Hence, Equation (A11) may be approximated as

$$\Psi_{\text{MSRSD-USTLD}} \lesssim \left(\mathrm{m}^2 + \mathrm{K}(\lambda-1)^{\mathrm{N_{Tx}}}\right)(16\mathrm{N_{Tx}N_{Rx}} + 8\mathrm{N_{Rx}} - 1). \tag{A12}$$